Review on Synthesis and Characterization of BiFeO3 Multiferroic Applications

Kishun Bir
Assistant Professor Department of Physics Kisan PG College Bahraich 271801 UP

1.INTRODUCTION

The compound BiFeO3 has a rhombohedral, pseudoperovskite, structure with alternating layers of bismuth and oxygen and iron and oxygen. The octahedral positions contain Fe3+ ions which cause exchange interaction between the Fe3+ ions along the Fe3+ – O2- – Fe3+ chains.

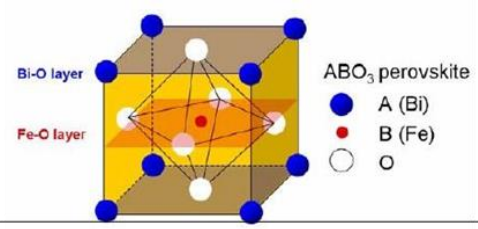

Fig.1 Schematic of the unit cell of $BiFeO_3$ which has the ABO_3 type perovskite

To meet the increasingly stringent demand for memory with improved energy efficiency, speed, and robustness, devices based on multiferroic complex metal oxides have been proposed as a potential route for spintronic memory.

Multiferroics are defined within this context for materials in which there is a coexistence and coupling of ferroelectric and magnetic ordering parameters. the development of devices and technological applications.

literature on BiFeO3 thin film growth, methods such as pulsed laser deposition (PLD), sputtering, or chemical vapour deposition (CVD) are reported, but these all require deposition temperatures in excess of 600 °C. On the other hand, atomic layer deposition has been shown to be a viable method for complex oxide growth at greatly reduced temperatures and is compatible for integration in large area wafers of 300 mm and larger.

2.EXPERIMENTAL PROCEDURE

2.1 Pulsed Laser Deposition

2.1.1 Fabrication of Thin Film

For the thin film fabrication, pulsed laser deposition (PLD) was used for the growth of the oxide thin films, and physical vapor deposition (PVD) was used for the growth if the magnetic or conducting metal thin films. A PLD system includes a laser source such as an ArF, KrF, or XeF excimer laser or a Nd:YAG laser, an optical system which contains an aperture, a mirror, and a focusing lens. It also includes a vacuum chamber which has a heater, a heating stage, a rotating target holder, and a moving shadow mask inside.

During the deposition process, the pulsed laser beam is focused onto a target to increase the laser energy density (energy/unit area at target surface) by a focusing lens. Typically the laser energy is in the range between 0.01 to 1.2 J at a frequency of 1 – 20 Hz during deposition. For the deposition of oxide thin films, oxygen must be introduced into the chamber in order to assist in the formation of the desired phase and obtain the correct film composition. The most important advantage of PLD is its versatility. Using the PLD technique, various materials such as oxides, semiconductors, and polymers can be easily grown. In general, the conditions are optimized to achieve stoichiometric transfer of the target composition to the film. Another advantage of PLD is the easy optimization process compared to other deposition techniques. Because of the short duration and high energy of the laser pulse, the target material plume is directed toward the substrate and different elemental components can have similar deposition rates, which help to make films with the same composition as the target.

In a combinatorial PLD chamber, the most important feature is the moving shadow mask located in front of a sample stage which allows the growth of films with gradients in the composition and/or thickness. The mask has a 10 × 10 mm square hole which is typically the same size as most commercial oxide substrates. By moving the shadow mask to cover and expose the

substrate to the deposition plume, each position in the sample can have different exposure time to the plume, and this results in continuously varied compositions across one sample. Such a sample is called a composition spread. Also using a single target, one can easily make samples with a thickness gradient which is a very useful technique to study microstructural evolution during film growth or the change of physical properties as a function of heteroepitaxial constraint.

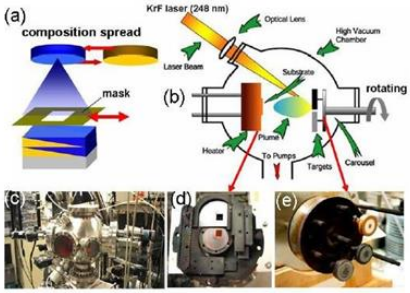

Fig..1 Schematics of (a) combinatorial pulsed laser deposition and (b) PLD system, which consists of (c) the chamber, (d) moving shadow mask, sample stage, and (e) multiple target stage.

2.1.2. Multiphase formation in Bi-Fe-O thin films

BiFeO3 has the advantage that its magnetic and ferroelectric transitions are above room temperature; the small magnetization (from canted antiferromagnetism) and significant leakage current density are significant problems for practical applications. In the Bi-Fe-O system, there are several phases of different structures, compositions, and electrical and magnetic properties which can co-exist. In some BiFeO3 thin films, improved magnetic properties were observed in an earlier study caused by a change of spiral magnetic spin through epitaxial constraint.

The change in magnetization with thickness for films grown at 5 mTorr and 20 mTorr oxygen partial pressures. Pure BiFeO3 films grown at 20 mTorr having thickness of 35 nm showed magnetization of about 5 emu/cc.

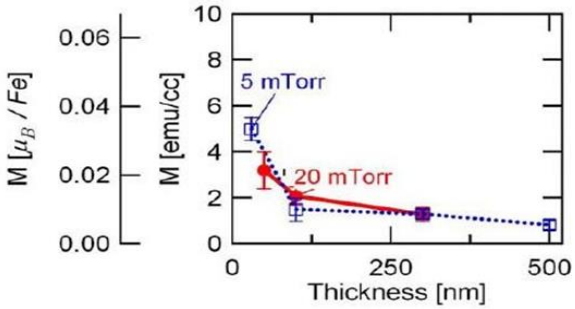

Fig. Room temperature saturation magnetization (emu/cc) of Bi-Fe-O films as a function of thickness for films grown at 5 mTorr and 20 mTorr.

2.2. Atomic Layer Deposition

Atomic layer deposition (ALD) is a thin film growth technique which has quickly become useful in both science and technology for the fabrication of high-quality ultrathin films. The technique consists of alternating half-reactions between a cation precursor and an anion precursor which are both self-limiting.

These aspects make the growth of BiFeO3 via ALD attractive because one can potentially coat three-dimensional nanoscale geometries with a conformal film, enabling unique composite multiferroic structures that could yield increased magnetoelectric coupling, such as embedded nanoparticles, embedded nanopillars, and nanolaminates. Despite this, there have been only a few demonstrated examples of BiFeO3 growth via ALD and no reports of plasma or radical-assisted ALD thus far.

2.2.1 Experimental Procedure

The multibeam system used in this study consists of a 10 in.-outer diameter stainless steel main chamber along with a load-lock assembly to facilitate sample insertion and removal without exposing the entire system to atmosphere. Affixed to the main chamber ports are several components: a coaxial microwave cavity radical beam source used to introduce highly reactive oxygen radicals to the sample, a six precursor doser array used to introduce evaporated organometallic precursor fluxes to the sample, a temperature-controlled sample stage, and a hot filament ion gauge which was used to measure the chamber pressure.

These are solid at room temperature and were sublimed at 150 and 130 °C, respectively. Depositions were carried out from 190 to 230 °C. The substrates used were Si (001) during process optimization, followed by SrTiO3 (001) (MTI Corp.) and Nb:SrTiO3 (001) (0.7 wt %) (MTI Corp.) for the piezoresponse force microscopy (PFM) experiments. For BiFeO3 films deposited on SrTiO3 and

Nb:SrTiO3, specimens were removed from the chamber after deposition.

2.2.2. Multiferroic Properties of BiFeO3 films

BiFeO3 films could be attained by RE-ALD, it was possible to characterize their functional ferroelectric and magnetic behavior. Because of the quality of the 650 °C film deposited on SrTiO3 (001), confirmed by XRD and TEM, the ferroelectric response was studied by PFM using a sister sample deposited using the same protocol on a Nb:SrTiO3 (001) (0.7 wt %) substrate to act as a bottom electrode. As shown in Figure 3, ferroelectric domain switching was demonstrated by locally applying ±12 V to reversibly write a square pattern into the domains as shown in Figure 4. The phase contrast confirmed the film was ferroelectric. as shown in Figure 5, the same epitaxial BiFeO3 sample characterized by TEM and XRD was observed to be weakly ferromagnetic, as indicated by the well-formed magnetic hysteresis loop. The saturation magnetization, Ms, at room temperature (298 K) was ~27 emu/cm3, whereas the magnetic coercivity HC was ~0.063 kOe.

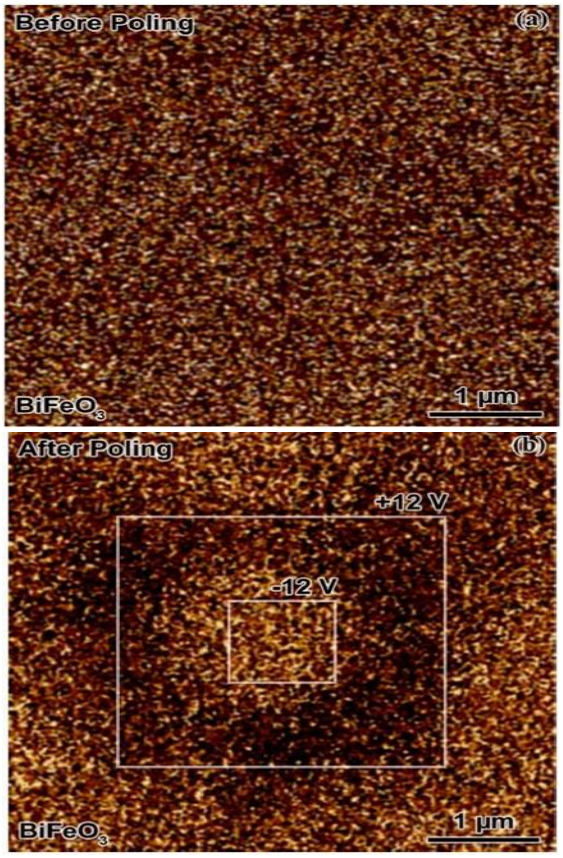

Piezoresponse force microscopy phase images of BiFeO3 film on Nb:SrTiO3 (001) substrate
(a) before(Fig.3) and (b) after ±12 V(Fig.4) applied using PFM tip in square pattern.

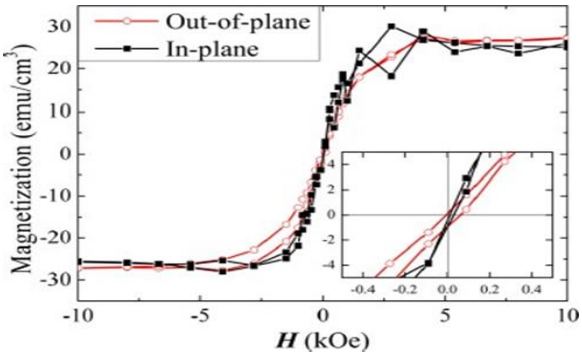

Fig.5. Magnetic hysteresis of BiFeO3 film annealed at 650 °C on SrTiO3 substrate with applied magnetic field oriented in-plane (black squares) and out-of-plane (red circles) relative to the film plane. Inset indicates zoomed view of magnetic coercivity.

3.CHARACTERIZATION

3.1Pulsed Laser Deposition

3.1.1.Transmission electron microscopy (TEM)

Transmission electron microscopy (TEM) was performed extensively to characterize the microstructure of the films. The morphological, crystallographic features as well as chemical information in the films have been obtained using TEM.

Fig. 6 shows TEM images of 200 nm thick bismuth iron oxide thin films grown at a

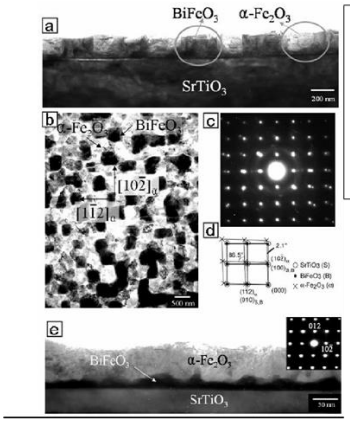

Fig.6

(a) Cross-sectional and (b) plan-view TEM images taken from a BiFeO3 film grown at 1 mTorr oxygen pressure, and (c) diffraction pattern and (d) indexing of plan-view diffraction pattern. e) Cross-sectional TEM image and electron diffraction (inset) from a BiFeO3 film grown at 0.1 mTorr oxygen pressure.

low oxygen partial pressure. BiFeO3 and Fe2O3 phases were found to have grown epitaxially with respect to the substrate as well as with respect to each other in the lateral direction in a columnar manner.
Fig.6(e) shows a BiFeO3 thin film fabricated at 0.1 mTorr. At this low pressure, the dominant h s s α-Fe2O3 which forms a continuous layer on a thin layer(5 nm) of BiFeO3 above the substrate.

3.1.2 XRD Analysis

Figure 7 shows x-ray diffraction (XRD) spectra of a series of bismuth iron oxide thin films deposited under different oxygen pressures. Epitaxial and pure BiFeO3 films were obtained at oxygen pressures higher than 5 mTorr, and the intensity of the (002) diffraction peaks of the BiFeO3 increases as the pressure increases. At the oxygen pressure of 20 mTorr, single phase BiFeO3 shows a monoclinically distorted (by about 0.5°) tetragonal structure. The lattice constants of the BiFeO3 calculated from electron diffraction data (not shown) are a = 0.394 nm, c = 0.398 nm. As the oxygen pressure is reduced below 5 mTorr, peaks corresponding to the Fe2O3 h s s [(012) α-F 2O3 d (024) γ-Fe2O3] appeared, and the intensity of these peaks increases as the oxygen pressure decreases. This transition in the dominant phase reflects the change in the amount of Bi incorporation in the films due to the high volatility of Bi.

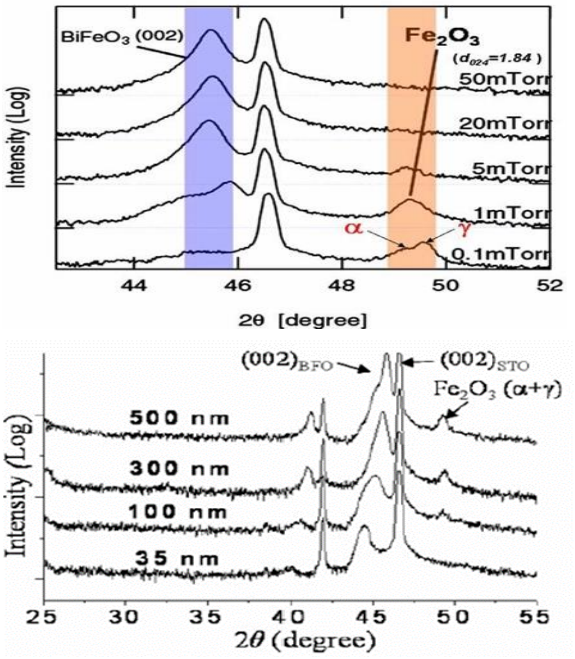

Fig.7 XRD spectra from BiFeO3 films grown at different deposition oxygen pressures

3.1.3. Magnetic Force Microscopy (MFM)

The magnetic domain image of the annealed multiphase Bi-Fe-O film was acquired s MFM h x s d s (γ-Fe2O3) after annealing. The magnetization of Bi-Fe-O film can be increased up to ~ 160 emu/cc wh α-F 2O3 s s γ-Fe2O3.

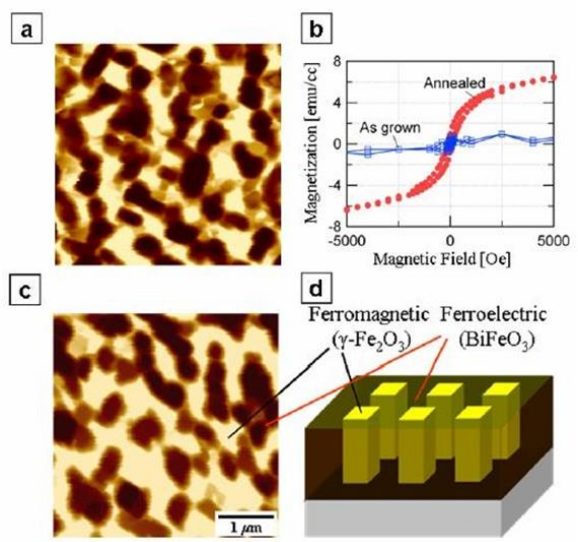

Fig. 8 Images of an annealed multiphase film (a) before and (c) after magnetizing the film perpendicular to the surface by applying 20 kOe magnetic field. (b) Hysteresis loops of as grown and annealed multiphase Bi-Fe-O films. (d) Schematic of the microstructure of Bi-Fe-O multiferroic nanocomposites.

3.2.Atomic Layer Deposition

3.2.1XPS Analysis

To confirm the initial synthesis of the desired constituent oxides Fe2O3 and Bi2O3 XPS was used. Figure 9 shows results for the films deposited at 210 °C on Si (001), consisting of 100 cycles of the ALD sequence with parameters of 90 s metalorganic precursor, 5 s pump-down, 20 s oxygen radical exposure, and 5 s pump-down. XP spectra were corrected to the accepted literature value of 284.8 eV for C 1s. As expected, the high- resolution XPS spectra for Fe 2p, seen in Figure 9a, displayed the spin orbital doublets 2p3/2 and 2p1/2, with peak positions at approximately 710.7 and 724.0 eV, respectively. For Bi2O3 seen in Figure 9b, the peak positions for Bi 4f7/2 and 4f5/2 were 158.6 and 163.9 eV, respectively, which indicated the Bi3+ oxidation state.

For Fe2O3, the deposition rate was relatively consistent, increasing slightly from 0.40 to 0.49 Å/cycle within the range of temperatures studied. For the composition of our Fe2O3 as a function of the deposition temperature, shown in Figure 9b, the proportions between Fe, O, and C did not vary significantly, with the Fe content fairly consistent between 30−32% and the C content between ∼17−20% with no obvious trend corresponding to the deposition rate.

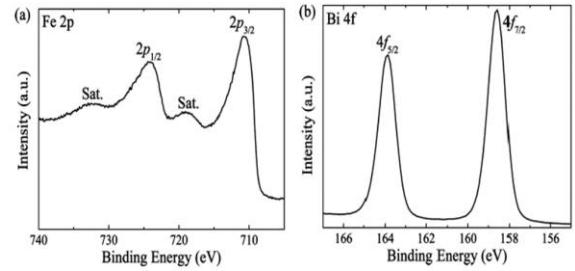

Fig 9. High resolution XPS spectra for (a) the Fe 2p peak from the Fe2O3 film and (b) the Bi 4f peak from the Bi2O3 film grown by ALD, both on Si (001).

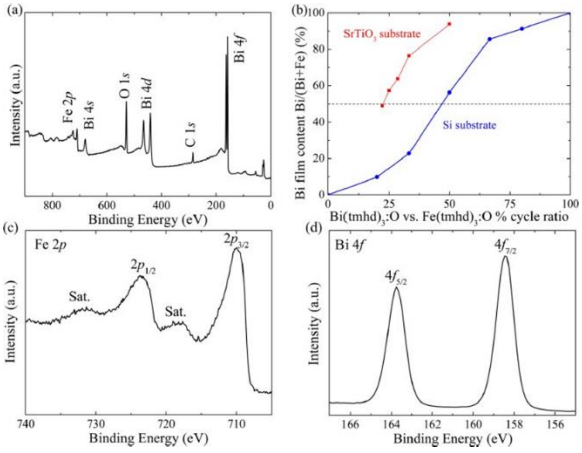

Fig.10. (a) XPS survey scan for BiFeO3 thin film grown by RE-ALD on Si (001). (b) Bismuth cation percentage (Bi/(Bi + Fe)%) of Bi2O3−Fe2O3 films on Si(001) and SrTiO3 (001) substrates as a function of pulse sequence percent ratio between Bi2O3 and Fe2O3 (defined as 100% × a/(a + b),where a and b are the number of Bi(TMHD)3:O and Fe(TMHD)3:O cycles, respectively). Detailed XPS spectra for (c) Fe 2p (Sat. indicates satellite peaks) and (d) Bi 4f photoelectron peaks.

3.2.2XRD Analysis

The BiFeO3(001)pc/SrTiO3 (001) crystallization process by RTA was optimized by varying s (450−750 °C) under oxygen for 60 s and a 50 °C/s ramp. Crystallinity, phasepurity, orientation, and texture were then analyzed as a function of the crystallization temperature using XRD as shown in Figure 11a. BiFeO3 films deposited at 210 °C before RTA consisted of a s α-Bi2O3, as indicated by its (012) reflection (28.01°, indicated on plot), which persisted up to crystallization temperatures of 450 °C. Low temperature ys z α-Bi2O3 has been reported previously in .28 Ab v 550 °C, h α-Bi2O3 reflection diminished and the reflections from BiFeO3 became prominent, in s h s d b d x (2θ = 22.4° (001)pc, 45.8° for (002)pc). Their highest intensity was observed for the 650 °C film. A detailed view of the BiFeO3 (001)pc peak is shown in Figure 11b for the 550 and 650 °C films. A change in the peak position as a function of film thickness was not detected up to 93.5 nm.

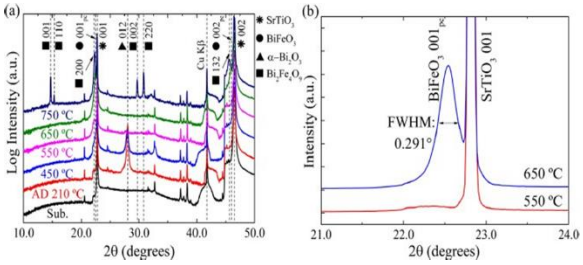

Fig 11.(a) Diffraction patterns for 35 nm thick BiFeO3 films grown on SrTiO3 (001) substrates as prepared and as a function of annealing temperature. Vertical lines indicate references from powder samples (PDF: BiFeO3 071-2494, α-Bi2O3 071−-2274, Bi2Fe4O9 025-0090, SrTiO3 086- 0178). (b) Detailed look at BiFeO3 (001)pc reflection for samples annealed at 550 and 650 °C.

4.CONCLUSION

The ferroelectric and ferromagnetic properties in multiferroic BiFeO3 thin films were investigated. The heteroepitaxial constraint created in a film structure by the substrate and the volatile nature of bismuth cause complicated changes to the microstructure and physical properties of BiFeO3 films. Secondary phases, such as, α-Fe2O3, γ-Fe2O3, and Fe3O4 formed spontaneously in the films grown at either relatively high growth temperature or low oxygen pressure. The formation of γ-Fe2O3 and Fe3O4 significantly increased the saturation magnetization of the films.

The ferroelectricity of BiFeO3 was studied in films with columnar structure of BiFeO3-Fe2O3 as well as films with polycrystalline BiFeO3. Both of them showed larger electrical polarization as well as less or no misfit strain compared to single crystalline epitaxial films with single BiFeO3 phase.

Epitaxial BiFeO3 thin films were synthesized using a radical enhanced atomic layer deposition (RE-ALD), with stoichiometry controlled toward unity by adjusting the precursor cycle sequence based on XPS. Crystallization of BiFeO3/SrTiO3 (001) was obtained by RTA from 550 to 650 °C epitaxy of the BiFeO3 was confirmed by combined XRD and TEM with an orientation relationship of BiFeO3 {001}pc‖SrTiO3 (001) and BiFeO3 ⟨100⟩pc‖SrTiO3 (100). The surface roughness increased from 3.8 Å before RTA to 44.8 Å after RTA at 650 °C.

REFERENCES

[1] W. Eerenstein, N. D. Mathur, and J. F. Scott, Nature 442, 759 (2006).
[2] E. Fischer, G. Gorodetsky and R. M. Hornreich, Solid State Commun. 10, 1127 (1972).
[3] L sk, M., M. Atomic Layer Deposition Chemistry: Recent Developments and Future Challenges. Angew. Chem., Int. Ed. 2003, 42, 5548−5554.
[4] Eerenstein, W.; Mathur, N. D.; Scott, J. F. Multiferroic and magnetoelectric materials. Nature 2006, 442, 759−65.
[5] Bibes, M.; Barthelemy, A. Multiferroics: Towards a magnetoelectric memory. Nat. Mater. 2008, 7, 425−426.